

Complex Gaussian Ratio-Based Bit Error Probability Calculation for PAM-FBMC Systems

Qiang Guo^{ID}, Ying Wang^{ID}, Jianhong Xiang^{ID}, and Yu Zhong^{ID}

Abstract—The interference induced by doubly-selective channels does not follow a Gaussian distribution, which leads to an inaccurate prediction for the reliability of Pulse Amplitude Modulation-based Filter Bank Multi-Carrier (PAM-FBMC) systems. In this letter, we derive a closed-form expression for the Bit Error Probability (BEP) based on Complex Gaussian Ratio (CGR), which accurately predicts the Bit Error Rate (BER) of the system and provides a basis for system design. Specifically, we first investigate the distribution properties of the ratio between the received symbol and the channel coefficients (i.e., CGR) to derive its joint probability density function. Secondly, based on the joint probability density of the CGR, we derive its Cumulative Distribution Function (CDF). Finally, we calculate the marginal CDF and, in conjunction with the decision boundaries provided by the PAM constellation, derive the BEP. Simulation results show that the CGR-based BEP provides a better agreement with the simulated BER.

Index Terms—PAM-FBMC, bit error probability, complex Gaussian ratio, bit error rate.

I. INTRODUCTION

FUTURE communications should support techniques such as immersive smart cities, smart vehicular networks, etc. The wireless channel for such communication cases is highly under spread [1]. Filter bank multi-carrier (FBMC) systems become a possible scheme [2]. FBMC supports asynchronous access and provides higher robustness to carrier frequency offset [3]. Moreover, it becomes an important R&D technique for future wireless systems because of its properties such as lower out-of-band emission and requiring no strict synchronization [4], [5], [6]. In time-varying multipath propagation (i.e., time-selective fading and frequency-selective fading), FBMC reliability is degraded. Thus, accurately predicting the reliability of FBMC in doubly selective channels becomes a crucial research area [1], [7], [8].

An important evaluation metric for predicting the reliability of FBMC in doubly selective channels is Bit Error Probability (BEP). Rugini and Banelli [9] investigated BEP for OFDM

Manuscript received 5 January 2024; revised 24 January 2024; accepted 1 February 2024. Date of publication 5 February 2024; date of current version 11 April 2024. This work is supported by Fundamental Research Funds for the Central Universities, China [3072022CF0801], Collaborative Research on Key Technologies for Maritime Search and Positioning Based on the BeiDou Navigation System, China [2018YFE0206500], and Sichuan Provincial Key Laboratory of Agile Intelligent Computing Project Fund. The associate editor coordinating the review of this letter and approving it for publication was A. Kaushik. (*Corresponding author: Jianhong Xiang*)

Qiang Guo, Ying Wang, and Jianhong Xiang are with the College of Information and Communication Engineering, Harbin Engineering University, Harbin 150001, China (e-mail: guoqiang@hrbeu.edu.cn; wangyingstu@163.com; xiangjianhong@hrbeu.edu.cn).

Yu Zhong is with the Agile and Intelligent Computing Key Laboratory, China Electronic Technology Group (Cetc-10), Chengdu 610036, China (e-mail: jade.zhong@hotmail.com).

Digital Object Identifier 10.1109/LCOMM.2024.3362332

systems in frequency selective fading. Wang et al. [10] studied the performance for OFDM systems in doubly selective fading. However, these methods cannot be directly applied to FBMC systems. The reason is that the orthogonality of FBMC holds only in real domain, which leads to inherent imaginary interference. Moreover, the related theoretical research on the BEP of FBMC systems is scarce. Nissel et al. [8] investigated the BEP performance of FBMC-OQAM and OFDM in doubly selective channels. This research provides an important contribution to the BEP calculation for FBMC systems. Particularly, Andrade et al. [7] investigated the BEP performance of QAM-FBMC in AWGN and Rayleigh fading channels. However, the implementation of QAM and OQAM modulation requires more complex algorithms and hardware. Pulse Amplitude Modulation (PAM) offers advantages such as low hardware implementation costs and high real-time performance (without involving complex phase modulation) [11]. Russell and Stuber [12] considered the issue of interference. They assumed that the interference follows a Gaussian distribution and applied the central limit theorem. However, the assumption is impractical because interferences are generally non-Gaussian distributed [8]. The above defects inspire and motivate us to research the BEP performance of PAM-FBMC. The novel contributions are summarized below:

- Based on the Complex Gaussian Ratio (CGR), we derive the BEP expression for the PAM-FBMC system. According to the property of PAM symbol set presenting a uniform distribution, we obtain the optimal decision boundary. Then, combining the decision boundary with the distributional properties of CGR, we complete the accurate calculation of BEP.
 - We derive the Cumulative Distribution Function (CDF) of the CGR. According to the Gaussian distribution property of CGR, we derive its probability density function and obtain the CDF. Then, we calculate biaxial (i.e., real-axis and imaginary-axis) marginal CDFs to improve the fitness of the decision boundary, and thus improve the BEP computational accuracy.
 - We adopt the 3GPP 38.900 channel model to verify the validity of our derivation. Compared to the Gaussian approximation, our derivation better matches the simulated BER perfectly (i.e., the error is less than 10^{-7}).
- Notations:* \otimes denotes the Kronecker product. $(\cdot)^*$, $(\cdot)^{-1}$, $(\cdot)^T$ and $(\cdot)^H$ denote the complex conjugation, inverse, transposition, and conjugate transposition, respectively.

II. SYSTEM MODEL

In FBMC, the transmitted signal comprises a set of interleaved PAM symbols, with symbol spacing shorter than their duration. We replace one QAM symbol by transmitting

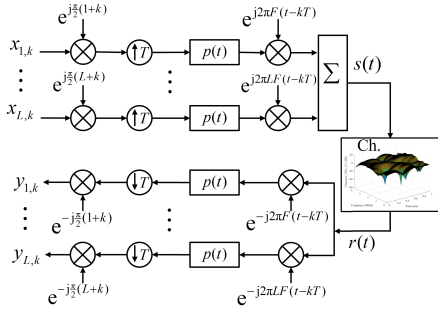


Fig. 1. Block diagram for the transmission structure of the system.

two interleaved PAM symbols, which ensures the spectral efficiency of the system. Meanwhile, to guarantee proper orthogonality (real orthogonality) among symbols, we need to introduce a phase shift factor between each symbol. Assuming the transmitted signal $s(t)$ is composed of L subcarriers and K time symbols, it can be expressed as

$$s(t) = \sum_{l=1}^L \sum_{k=1}^K x_{l,k} \underbrace{p(t - kT) e^{j2\pi lF(t-kT)} e^{j\pi(l+k)/2}}_{g_{l,k}(t)}. \quad (1)$$

where $x_{l,k}$ denotes the transmitted symbol at time-frequency position (l, k) , selected from the PAM symbol alphabet χ . F denotes the frequency spacing and T the time spacing. $p(t)$ denotes the prototype filter and $e^{j\pi(l+k)/2}$ the phase shift factor. $g_{l,k}(t)$ denotes the base pulse. The received signal $r(t)$ can be characterized by convolving $s(t)$ with the time-varying multipath channel, denoted by

$$\begin{aligned} r(t) &= \int_{\mathbb{R}} s(\tau) h(t, \tau) d\tau + n(t) \\ \text{st. } h(t, \tau) &= \frac{1}{\sqrt{P}} \sum_{p=1}^P \eta_p(t) e^{j(f_{Dp} + \varphi_p)} \delta_{\tau - \tau_n}. \end{aligned} \quad (2)$$

where P denotes the number of paths and $\eta_p(t)$ the attenuation factor of the p -th path. f_{Dp} and φ_p denote the Doppler shift and initial phase, respectively. δ denotes the Kronecker delta function. $n(t)$ denotes white noise. Adopting matched filtering, we can determine the received symbol $y_{l,k}$ at time-frequency position (l, k) , denoted as

$$y_{l,k} = \int_{\mathbb{R}} r(t) g_{l,k}^*(t) dt. \quad (3)$$

For the k -th symbol, the transmission structure of the system is shown in Fig. 1. The condition of real orthogonality determined by the phase shift factor can be expressed as

$$\Re \left\{ \int_{\mathbb{R}} g_{l,k}(t) g_{l',k'}^*(t) dt \right\} = \delta_{\Delta l, \Delta k}. \quad (4)$$

where $\Delta l = l - l'$ and $\Delta k = k - k'$. However, real orthogonality leads to imaginary interference. For precise analysis, we define the interference term as

$$\zeta_{l,k}^{l',k'} = \int_{\mathbb{R}} g_{l,k}(t) g_{l',k'}^*(t) dt. \quad (5)$$

Note that if $(l, k) = (l', k')$, then $\zeta_{l,k}^{l',k'} = 1$; if $(l, k) \neq (l', k')$, then $\zeta_{l,k}^{l',k'}$ is purely imaginary. Due to the high under-

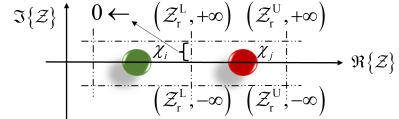


Fig. 2. Decision boundaries for PAM alphabet symbol χ_j . When offset of χ_j exceeds the upper bound Z_r^U or the lower bound Z_r^L , the judgment of the other symbols is impacted. Note that the arrow pointing to 0 indicates that the horizontal decision boundary tends to 0.

spreading in wireless channels [1], received symbols can be effectively characterized by one-tap channels. Thus, Eq. (3) can be rewritten as

$$y_{l,k} = H_{l,k} x_{l,k} + \sum_{l' \neq l} \sum_{k' \neq k} H_{l',k'} x_{l',k'} \zeta_{l,k}^{l',k'} + n_{l,k}. \quad (6)$$

where $H_{l,k}$ denotes the one-tap channel at time-frequency position (l, k) , and $n_{l,k} = \int_{\mathbb{R}} n(t) g_{l,k}^*(t) dt$ the noise term.

To simplify Eq. (6), we consider the system description in matrix form. We adopt the rate f_s to sample the base pulse at N points and express the samples by the vector $\mathbf{g}_{l,k} \in \mathbb{C}^{N \times 1}$. Then, all the vectors are integrated into the transfer matrix $\mathbf{G} = [\mathbf{g}_{1,1}, \dots, \mathbf{g}_{L,K}] \in \mathbb{C}^{N \times LK}$. The global system model can be expressed as [13]

$$\mathbf{y} = \mathbf{G}^H \mathbf{HG} \mathbf{x} + \mathbf{n}. \quad (7)$$

where $\mathbf{x} = [x_{1,1}, \dots, x_{L,K}]^T \in \mathbb{C}^{LK \times 1}$ denotes the transmitted symbol and $\mathbf{y} = [y_{1,1}, \dots, y_{L,K}]^T \in \mathbb{C}^{LK \times 1}$ the received symbol. $\mathbf{n} \sim \mathcal{CN}(\mathbf{0}, P_n \mathbf{G}^H)$ denotes the complex Gaussian noise with power P_n , and $\mathbf{H} \in \mathbb{C}^{N \times N}$ the channel convolution matrix [13]. And $H_{l,k}$ in Eq. (6) is calculated as

$$H_{l,k} = \sum_{n=1}^N [(g_{l,k}^H \mathbf{H}) \circ g_{l,k}^T]_n. \quad (8)$$

where \circ denotes the Hadamard product. Note that the interference term in Eq. (6) is described as off-diagonal elements of $\mathbf{G}^H \mathbf{HG}$.

III. BIT ERROR PROBABILITY

For real-valued PAM, the constellation points are only twisted or shifted on the real axis in one dimension. Thus, The PAM constellation requires only vertical decision boundaries, not horizontal ones, see Fig. 2. The PAM symbol set is uniformly distributed, enabling us to evenly divide the range of allowable offsets for accurate symbol detection. Therefore, we present the method for calculating BEP for PAM-FBMC.

Conditioned on the transmitted symbol x , the received symbol y (i.e., $y_{l,k}$) at any time-frequency position satisfies a Gaussian distribution [8]. We assume that the channel coefficient H (i.e., $H_{l,k}$) satisfies a complex Gaussian distribution, which is reasonable in multipath transmission [14]. Thus, y and H have joint density [15], expressed as

$$f_{y,H}(y, H) = \frac{1}{\pi^2 |\mathbb{E}|} \exp \left(- \left[\begin{bmatrix} y \\ H \end{bmatrix} \right]^H \mathbb{E}^{-1} \left[\begin{bmatrix} y \\ H \end{bmatrix} \right] \right). \quad (9)$$

where

$$\mathbb{E} = \begin{bmatrix} \mathbb{E}\{y^*y\} & \mathbb{E}\{y^*H\} \\ \mathbb{E}\{yH^*\} & \mathbb{E}\{H^*H\} \end{bmatrix} = \begin{bmatrix} \sigma_y^2 & \rho\sigma_y\sigma_H \\ \rho^*\sigma_y\sigma_H & \sigma_H^2 \end{bmatrix}. \quad (10)$$

The theory for complex Gaussian variables can be referred to [15]. Note that $\rho = \rho_r + j\rho_i$ is complex-valued, and the complex Gaussian ratio $\mathcal{Z} = y/H = \mathcal{Z}_r + j\mathcal{Z}_i$ has the probability density function, denoted as

$$f_{y/H}(\mathcal{Z}_r, \mathcal{Z}_i) = \frac{1 - \rho^2}{\pi\sigma_y^2\sigma_H^2} \left(\frac{\mathcal{Z}^2}{\sigma_y^2} + \frac{1}{\sigma_H^2} - 2\frac{\rho_r\mathcal{Z}_r - \rho_i\mathcal{Z}_i}{\sigma_y\sigma_H} \right)^{-2}. \quad (11)$$

See appendix for proof. Typically, to assess the fading channel, we require deriving the BEP of AWGN and then integrating the channel density function [16]. Therefore, adopting the joint density helps to calculate the BEP for doubly selective channels. The integral of Eq. (11) reads

$$\begin{aligned} \mathcal{G}(\mathcal{Z}_r, \mathcal{Z}_i) &= \iint f_{y/H}(\mathcal{Z}_r, \mathcal{Z}_i) d\mathcal{Z}_r d\mathcal{Z}_i \\ &= \Pi(\mathcal{Z}_r, \mathcal{Z}_i, \rho_r, \rho_i) + \Pi(\mathcal{Z}_i, \mathcal{Z}_r, -\rho_i, -\rho_r). \end{aligned} \quad (12)$$

where

$$\begin{aligned} \Pi(\mathcal{Z}_r, \mathcal{Z}_i, \rho_r, \rho_i) &= \frac{\rho_i\sigma_y + \sigma_H\mathcal{Z}_i}{2\pi\sqrt{\psi(\mathcal{Z}_i, \rho_r, \rho_i)}} \tan^{-1} \left(\frac{\sigma_H\mathcal{Z}_r - \rho_r\sigma_y}{\sqrt{\psi(\mathcal{Z}_i, \rho_r, \rho_i)}} \right), \end{aligned} \quad (13)$$

$$\begin{aligned} \Pi(\mathcal{Z}_i, \mathcal{Z}_r, -\rho_i, -\rho_r) &= \frac{-\rho_r\sigma_y + \sigma_H\mathcal{Z}_r}{2\pi\sqrt{\psi(\mathcal{Z}_r, -\rho_i, -\rho_r)}} \tan^{-1} \left(\frac{\sigma_H\mathcal{Z}_i + \rho_i\sigma_y}{\sqrt{\psi(\mathcal{Z}_r, -\rho_i, -\rho_r)}} \right), \end{aligned} \quad (14)$$

with

$$\psi(\mathcal{Z}_i, \rho_r, \rho_i) = (1 - \rho_r^2)\sigma_y^2 + 2\rho_i\sigma_y\sigma_H\mathcal{Z}_i + \sigma_H^2\mathcal{Z}_i^2, \quad (15)$$

$$\psi(\mathcal{Z}_r, -\rho_i, -\rho_r) = (1 - \rho_i^2)\sigma_y^2 - 2\rho_r\sigma_y\sigma_H\mathcal{Z}_r + \sigma_H^2\mathcal{Z}_r^2. \quad (16)$$

According to Eqs. (12)-(16), the CDF of the complex Gaussian ratio \mathcal{Z} can be expressed as

$$\begin{aligned} \mathcal{F}_{y/H}(\mathcal{Z}_r, \mathcal{Z}_i) &= \mathcal{G}(\mathcal{Z}_r, \mathcal{Z}_i) + \frac{1}{4} \left(\frac{\sigma_H\mathcal{Z}_i + \rho_i\sigma_y}{\sqrt{\psi(\mathcal{Z}_i, \rho_r, \rho_i)}} \right. \\ &\quad \left. + \frac{\sigma_H\mathcal{Z}_r - \rho_r\sigma_y}{\sqrt{\psi(\mathcal{Z}_r, -\rho_i, -\rho_r)}} + 1 \right). \end{aligned} \quad (17)$$

Generally, we only need to calculate the real-axis marginal CDF [1], [8], which corresponds to the probability that the real part of \mathcal{Z} is less than the decision threshold \mathcal{Z}_R . According to Eq. (17), we can calculate $\Pr(\Re\{\mathcal{Z}\} < \mathcal{Z}_R)$ as

$$\begin{aligned} \Pr(\Re\{\mathcal{Z}\} < \mathcal{Z}_R) &= \lim_{\mathcal{Z}_i \rightarrow \infty} \mathcal{F}_{y/H}(\mathcal{Z}_R, \mathcal{Z}_i) \\ &= \frac{1}{2} + \frac{\sigma_H\mathcal{Z}_R - \rho_R\sigma_y}{2\sqrt{\psi(\mathcal{Z}_R, -\rho_I, -\rho_R)}}. \end{aligned} \quad (18)$$

For a given symbol alphabet χ , we consider the probability that the receiver detects $\hat{x}_{l,k} = \chi_j$ given that the transmitted symbol is $x_{l,k} = \chi_i$. The probability $\Pr(\hat{x} = \chi_j | x = \chi_i)$ can be calculated as

$$\Pr(\hat{x} = \chi_j | x = \chi_i)$$

$$\begin{aligned} &= \mathcal{F}_{y/H}(\mathcal{Z}_r^U, +\infty | \chi_i) + \mathcal{F}_{y/H}(\mathcal{Z}_r^L, -\infty | \chi_i) \\ &\quad - \mathcal{F}_{y/H}(\mathcal{Z}_r^L, +\infty | \chi_i) - \mathcal{F}_{y/H}(\mathcal{Z}_r^U, -\infty | \chi_i). \end{aligned} \quad (19)$$

The upper limit \mathcal{Z}_r^U and lower limit \mathcal{Z}_r^L of the real part decision threshold are denoted as

$$\mathcal{Z}_r^U = \max_{\chi_j} (\Re\{\chi\} | x = \chi_i). \quad (20)$$

$$\mathcal{Z}_r^L = \min_{\chi_j} (\Re\{\chi\} | x = \chi_i). \quad (21)$$

Currently, we are unable to calculate the BEP. The reason is that Eq. (19) still relies on the expectation value in Eq. (10). Conditioned on $\mathbf{x} \in \mathbb{C}^{LK \times 1}$, we can calculate the required expectation as

$$\begin{aligned} \mathbb{E}\{y_{l,k}^*y_{l,k}|\mathbf{x}\} &= |\mathbf{x}^T \mathbf{G}^T \mathbf{R} \mathbf{G}^* \mathbf{x}^*| + P_n \\ \mathbb{E}\{y_{l,k}H_{l,k}^*|\mathbf{x}\} &= \mathbf{x}^T \mathbf{G}^T \mathbf{R} \mathbf{g}_{l,k}^*. \end{aligned} \quad (22)$$

where $\mathbf{R} = (\mathbf{I}_N \otimes \mathbf{g}_{l,k})^H \mathbf{R}_H (\mathbf{I}_N \otimes \mathbf{g}_{l,k}) \in \mathbb{C}^{LK \times LK}$ with $\mathbf{R}_H = \mathbb{E}\{\text{vec}\{\mathbf{H}\} \text{vec}\{\mathbf{H}\}^H\}$ denotes the channel correlation matrix. $\mathbb{E}\{H^*H\}$ is independent of the data and noise, therefore, allowing us to calculate it as

$$\mathbb{E}\{H_{l,k}^*H_{l,k}\} = |(\mathbf{g}_{l,k}^T \otimes \mathbf{g}_{l,k}^H) \mathbf{R}_H (\mathbf{g}_{l,k}^* \otimes \mathbf{g}_{l,k})|. \quad (23)$$

Note that the parameters required for the computation in Eq. (18) can all be obtained through the ratio in Eqs. (22)-(23). And, Conditioned on the transmitted symbol \mathbf{x} , the expectation value we calculate can fully consider the channel-induced interference. Therefore, our scheme can more accurately predict the system reliability. Now, adopting Eq. (19), we can calculate the BEP, expressed as

$$\begin{aligned} \text{BEP}_{l,k} &= \frac{1}{\log_2 |\chi|} \sum_{\ell=1}^{\log_2 |\chi|} \frac{1}{|\chi|} \sum_{i=1}^{|\chi|} \sum_{\chi_j \in \bar{\chi}_i^\ell} \Pr(\hat{x}_{l,k} = \chi_j | x_{l,k} = \chi_i). \end{aligned} \quad (24)$$

where, the set $\bar{\chi}_i^\ell$ represents all elements different from χ_i at bit position ℓ . When the amount of data is large, Eq. (22) and Eq. (23) are computationally intensive. Specifically, the computational complexity for Eqs. (22) and (23) are $\mathcal{O}(NL^3K^3)$ and $\mathcal{O}(N^4)$, respectively. However, only symbols (about 4-8 [13]) close to $x_{l,k}$ have a significant impact on its BEP. Therefore, we can reduce the number of symbols considered to decrease the complexity.

IV. NUMERICAL RESULTS

In this section, we numerically evaluate the proposed BEP expression. We consider BEP performance in flat fading and time-varying multipath transmission. The simulated BER and the Gaussian interference approximation of the BEP [12] are considered for comparison. To evaluate the performance of PAM-FBMC in frequency-selective Rayleigh fading channels, several researchers have considered the “Extended Pedestrian A” and “Extended Vehicular A” channel models provided by 3GPP [5], [17]. Without loss of generality, we employ the channel models “Pedestrian A” and “Vehicular A” of 3GPP

TABLE I
MONTE CARLO SIMULATION PARAMETERS

Parameter name	Value
No. of subcarriers and symbols	$L = 128, K = 14$
Carrier frequency and frequency spacing	2.5 GHz, $F = 15$ kHz
Sampling rate	$f_s = 5.04$ MHz
Modulation order	{2, 4, 8, 16} – PAM
Prototype filter and overlap factor	PHYDYAS [19], 4

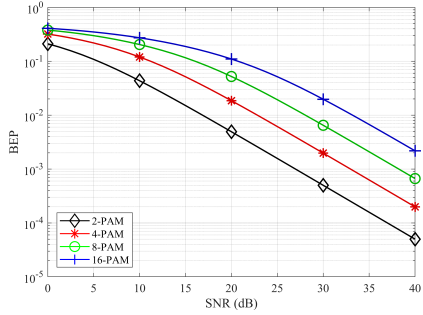


Fig. 3. BEP versus SNR in the case of flat fading. BEP performance is not related to the multicarrier scheme but to the modulation order. When SNR is less than 20 dB, the flat fading BEP can describe the doubly selective channel (see Fig. 4).

38.800 [18]. Firstly, we adopt the “Pedestrian A” channel model to simulate a flat channel with Root Mean Square (RMS) delay spread of 46 ns. Secondly, we adopt the “Vehicular A” channel model to approximate the doubly selective channel and set the RMS delay spread to 370 ns. Additionally, we consider the BEP at different velocities, which corresponds to the case of different latency spreads. Finally, for the PAM-FBMC system, The Monte Carlo simulation parameters we considered are listed in Table I.

Note that the minimum sampling rate for the system shall be $f_s = 2FL$. For the “Pedestrian A” channel model, we assign the number of Wide-sense Stationary Uncorrelated Scattering (WSSUS) paths to 50 and the velocity to 5km/h. Fig. 3 shows the relationship between BEP and SNR for the flat fading case. In high SNR case, BEP shows linear behavior. In flat channel $\mathbf{H} = \bar{h}\mathbf{I}_N$, FBMC experiences imaginary interference that does not impact BEP [8]. And the required expectations are $E\{y_{l,k}^*y_{l,k}|\mathbf{x}\} = |x_{l,k}|^2 + P_n$, $E\{y_{l,k}H_{l,k}^*|\mathbf{x}\} = x_{l,k}$ and $E\{H_{l,k}^*H_{l,k}\} = 1$, respectively. Thus, combining Eq. (18), we can provide an approximate result for Eq. (24) (in terms of 2-PAM), expressed as

$$\text{BEP}_{l,k}^{2-\text{PAM}} \approx \frac{1}{2} - \frac{1}{2\sqrt{2\left(1 + \frac{P_n\epsilon}{E\{|x_{l,k}|^2\}}\right)} - 1}. \quad (25)$$

where ϵ is a scalar value, usually 1. Note that the approximate result for Eq. (25) no longer applies to the doubly selective channel. Instead, it strictly relies on Eq. (24). In practical scenarios, the SNR is less than 20dB [8]. The BEP in the case of flat fading provides a valuable reference for doubly selective channels. For the “Vehicular A” channel model, we assign the number of WSSUS paths to 200 and the velocity to 200km/h. At this point, the coherence time and bandwidth of the channel are 0.82ms and 1.5MHz, respectively. Fig. 4 shows

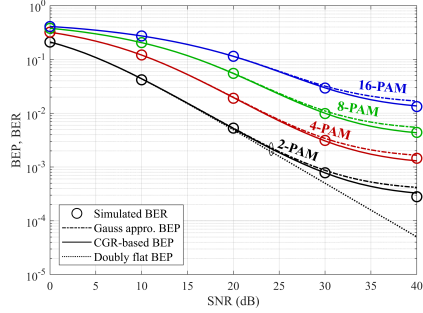


Fig. 4. BEP versus SNR in the case of doubly selective fading. When noise dominates, a flat-fading BEP can accurately describe the system performance.

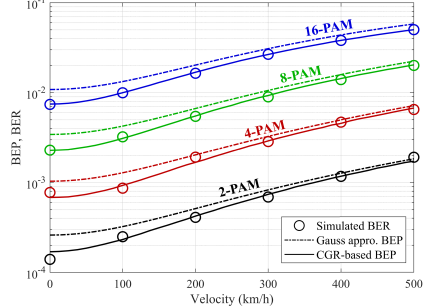


Fig. 5. BEP versus velocity in the noiseless case. In high-mobility environments, the interference is mainly dominated by the Doppler spread, and thus the Gaussian approximation has a large error (about 1%-5%).

the relationship between BEP and SNR for the doubly selective fading case. The noise follows a Gaussian distribution, but the interference does not. Thus, the Gaussian approximation has the same performance as the CGR-based BEP when noise is dominant (i.e., SNR is less than 20 dB). However, the Gaussian approximation is biased when interference dominates. At this point, the CGR-based calculation method can more accurately describe the system’s BEP.

Now, we consider a system with only interference (i.e., $\text{SNR} \rightarrow \infty$) and examine the relationship between BEP and velocity. Fig. 5 shows the BEP versus velocity for the noiseless case. For low mobility, frequency selective fading due to multipath transmission causes interference. This interference can be eliminated by reducing the bit rate. However, lowering the bit rate will lead to some deviation of the simulated BER from the CGR-based BEP (about 0.05%-1%). Compared to the Gaussian approximation, our scheme is more accurate. However, in highly frequency-selective fading channels, the CGR-based scheme exhibits prediction errors due to random fluctuations. In this case, our scheme may not perform optimally. Note that when the Mean Square Error (i.e., the error between the simulated and the analytical values) is within $(-15.27, -8.72)$ dB, the credibility of our scheme is 95%. In contrast, the Gaussian approximation has only 80% credibility. Credibility means the probability that the error value belongs to the confidence interval $(-15.27, -8.72)$ dB.

V. CONCLUSION

In this letter, we derived the BEP expression for the PAM-FBMC system. This method is implemented based on CGR. For high SNR (above 20 dB), our scheme is more accurate than Gaussian approximation and closer to the simulated values. Also, at low SNR (below 20 dB), our scheme also

accurately describes the BER of the system. The aim of the proposed method is to predict the BER of the PAM-FBMC system. The CGR-based approach is not only applicable to flat channels, but also helps to analyze the impact of time-varying multipath propagation. This provides an important basis for evaluating the reliability for the PAM-FBMC system. However, a more complex multi-antenna system has not been studied yet, and we plan to explore this in future work.

APPENDIX

CALCULATION OF THE PROBABILITY DENSITY FUNCTION FOR THE COMPLEX GAUSSIAN RATIO $\mathcal{Z} = y/H$

The correlated binary complex Gaussian variables in Eq. (9) can be written as $y = y_r + jy_i$ and $H = H_r + jH_i$, respectively [15]. When the binary complex Gaussian variables are zero-mean, the probability density function can be written as

$$\begin{aligned} f_{y,H}(y_r, y_i, H_r, H_i) &= \frac{1}{\pi^2 \sigma_y \sigma_H (1 - \rho^2)} \exp \left(\frac{-1}{1 - \rho^2} \times \left(\frac{y_r^2 + y_i^2}{\sigma_y^2} \right. \right. \\ &\quad \left. \left. + \frac{H_r^2 + H_i^2}{\sigma_H^2} - \frac{2\rho}{\sigma_y \sigma_H} (y_i H_i + y_r H_r) \right) \right). \end{aligned} \quad (26)$$

And the probability density function of $\mathcal{Z} = y/H$ can be calculated as

$$\begin{aligned} f_{y/H}(\mathcal{Z}) &= \int \int \int \int_{\mathbb{R}} f_{y,H}(y_r, y_i, H_r, H_i) \\ &\quad \times \delta \left(\frac{y_r + jy_i}{H_r + jH_i} - \mathcal{Z} \right) dy_r dy_i dH_r dH_i. \end{aligned} \quad (27)$$

where $\delta(\cdot)$ denotes the complex delta function. Adopting variables substitutions $y = uv$ and $H = v$ [20], we can simplify the probability density function of the complex Gaussian ratio. The substitution rules for complex values are $y = (u_r v_r - u_i v_i) + j(u_r v_i + u_i v_r)$ and $H = v_r + jv_i$. Thereby, the Jacobian determinant is $v_i^2 + v_r^2$. Thus, the CDF of \mathcal{Z} can be defined as

$$\begin{aligned} \mathcal{F}_{y/H}(\mathcal{Z}) &= \int_{-\infty}^{z_r} \int_{-\infty}^{z_i} \int_{-\infty}^{\infty} \int_{-\infty}^{\infty} (v_i^2 + v_r^2) f_{y,H}(u_r v_r - u_i v_i, u_r v_i \\ &\quad + u_i v_r, v_r, v_i) dv_r dv_i du_i du_r. \end{aligned} \quad (28)$$

Thereby, $f_{y/H}(z_r, z_i)$ can be calculated as

$$\begin{aligned} f_{y/H}(z_r, z_i) &= \frac{\partial^2}{\partial u_r \partial u_i} \mathcal{F}_{y/H}(z_r, z_i) \\ &= \int_{-\infty}^{\infty} \int_{-\infty}^{\infty} (v_i^2 + v_r^2) f_{y,H}(z_r v_r - z_i v_i, z_r v_i \\ &\quad + z_i v_r, v_r, v_i) dv_r dv_i. \end{aligned} \quad (29)$$

Combining Eq. (26) and Eq. (29), we transform the variables to polar coordinates to calculate the integral which yield Eq. (11).

REFERENCES

- [1] R. Nissel and M. Rupp, "Bit error probability for pilot-symbol aided channel estimation in FBMC-OQAM," in *Proc. IEEE Int. Conf. Commun. (ICC)*, May 2016, pp. 1–6.
- [2] G. Wunder et al., "5GNOW: Non-orthogonal, asynchronous waveforms for future mobile applications," *IEEE Commun. Mag.*, vol. 52, no. 2, pp. 97–105, Feb. 2014.
- [3] D. Mattera and M. Tanda, "Performance analysis of FBMC-PAM systems in frequency-selective Rayleigh fading channels in the presence of phase error," in *Proc. IEEE Int. Conf. Commun., Netw. Satell. (COMNETSAT)*, Nov. 2022, pp. 264–269.
- [4] Y. Qi, J. Dang, Z. Zhang, L. Wu, and Y. Wu, "Efficient channel equalization and performance analysis for uplink FBMC/OQAM-based massive MIMO systems," *IEEE Trans. Veh. Technol.*, vol. 72, no. 9, pp. 1–16, Sep. 2023, doi: 10.1109/TVT.2023.3263220.
- [5] M. Tanda, "Asymptotic performance of FBMC-PAM systems in frequency-selective Rayleigh fading channels," *Signal Process.*, vol. 201, Dec. 2022, Art. no. 108693.
- [6] H. Wang, L. Xu, Z. Yan, and T. A. Gulliver, "Low-complexity MIMO-FBMC sparse channel parameter estimation for industrial big data communications," *IEEE Trans. Ind. Informat.*, vol. 17, no. 5, pp. 3422–3430, May 2021.
- [7] I. Galdino Andrade, D. Le Ruyet, M. L. R. de Campos, and R. Zakaria, "Bit error probability expressions for QAM-FBMC systems," *IEEE Commun. Lett.*, vol. 26, no. 5, pp. 994–998, May 2022.
- [8] R. Nissel and M. Rupp, "OFDM and FBMC-OQAM in doubly-selective channels: Calculating the bit error probability," *IEEE Commun. Lett.*, vol. 21, no. 6, pp. 1297–1300, Jun. 2017.
- [9] L. Rugini and P. Banelli, "BER of OFDM systems impaired by carrier frequency offset in multipath fading channels," *IEEE Trans. Wireless Commun.*, vol. 4, no. 5, pp. 2279–2288, Sep. 2005.
- [10] T. Wang, J. G. Proakis, E. Masry, and J. R. Zeidler, "Performance degradation of OFDM systems due to Doppler spreading," *IEEE Trans. Wireless Commun.*, vol. 5, no. 6, pp. 1422–1432, Jun. 2006.
- [11] D. Mattera, M. Tanda, and M. Bellanger, "Filter bank multicarrier with PAM modulation for future wireless systems," *Signal Process.*, vol. 120, pp. 594–606, Mar. 2016.
- [12] M. Russell and I. Gordon, "Interchannel interference analysis of OFDM in a mobile environment," in *Proc. IEEE 45th Veh. Technol. Conf., Countdown Wireless*, Jul. 1995, pp. 820–824.
- [13] Y. Wang, Q. Guo, J. Xiang, and Y. Liu, "Doubly selective channel estimation and equalization based on ICI/ISI mitigation for OQAM-FBMC systems," *Phys. Commun.*, vol. 59, Aug. 2023, Art. no. 102120.
- [14] T. Rappaport, *Wireless Communications: Principles and Practice*. Upper Saddle River, NJ, USA: Prentice-Hall, 2001.
- [15] N. R. Goodman, "Statistical analysis based on a certain multivariate complex Gaussian distribution (an introduction)," *Ann. Math. Statist.*, vol. 34, no. 1, pp. 152–177, Mar. 1963.
- [16] J. G. Proakis, *Digital Communications*. New York, NY, USA: McGraw-Hill, 2008.
- [17] D. Mattera, M. Tanda, and M. Bellanger, "On the performance of FBMC-PAM systems in frequency-selective Rayleigh fading channels," *Phys. Commun.*, vol. 45, Apr. 2021, Art. no. 101264.
- [18] *Technical Specification—LTE*, Standard ETSI TS 136 213, V8. 8.0, T ETSI, 2010, pp. 136200–136299.
- [19] M. Bellanger et al., "FBMC physical layer: A primer," *PHYDYAS*, vol. 25, no. 4, pp. 7–10, Jan. 2010.
- [20] J. H. Curtiss, "On the distribution of the quotient of two chance variables," *Ann. Math. Statist.*, vol. 12, no. 4, pp. 409–421, Dec. 1941.